Geomechanics and Engineering, *Vol. 27, No. 2 (2021) 167-178*
https://doi.org/10.12989/gae.2021.27.2.167

Contribution of using geogrid under a shallow foundation on sand subjected to static and repeated loads: Laboratory testing and numerical simulations

Mustafa Tolun*[1], Sefer E. Epsileli[2a], Buse Emirler[3b], Abdulazim Yildiz[3c] and Erol Tutumluer[4d]

[1]*Department of Civil Engineering, Adana Alparslan Turkes Science and Technology University, 01250, Adana, Turkey*
[2]*6th Regional Directorate, Republic of Turkey General Directorate of Highways, 38060, Kayseri, Turkey*
[3]*Department of Civil Engineering, Cukurova University, 01250, Adana, Turkey*
[4]*Department of Civil and Environmental Engineering, University of Illinois at Urbana-Champaign, Illinois, 61801, U.S.A.*

(Received October 12, 2020, Revised October 4, 2021, Accepted October 7, 2021)

Abstract. This paper focuses on the use of a certain punched and drawn geogrid to increase the bearing capacity of a circular shallow foundation subjected to a combination of static and repeated loads. In the experiments, the foundation is first subjected to a prespecified static load, afterwards, a repeated load derived in different proportions of the applied static load is superimposed to that static load. The variables investigated in the tests are the number of geogrid layers, the amplitude of repeated load, and the number of load cycles. The effect of these variables is also investigated by a finite element numerical modeling approach verified with one-dimensional site response analysis, and as a consequence of this effort that refers to the innovation of the study, the consistency between the results obtained from both methods is observed. The test results show that the displacements of the shallow foundation increase rapidly in the first 100 load cycles in all cases. After that, the rate of increase is reduced until about 2000 load cycles and the displacements become negligible. From the experiments, 2 geogrid layers were found to be quite effective in reducing displacements due to both static and dynamic loading cases. In other respects, finite element simulations of the physical experiment have produced numerical results in good agreement with the test results. Plus, the main contribution of the numerical simulation is to indicate the deformed mesh outputs of the model including the geogrids for the foregoing variables.

Keywords: finite element method; geogrid-reinforcement; large-scale test; repeated loading; shallow foundation

1. Introduction

Quite a few geotechnical cases occur in which the foundations of structures are subjected to static loading as well as repeated loading. Road embankments under repeatable traffic loads and machine foundations under vibration are examples of such foundations where the repeated loads bring about to decrease the bearing capacity of these foundations. The soils under these sorts of foundations can be reinforced with geosynthetics to improve their engineering properties and therefore their bearing capacities. Geosynthetics have been used for a long time in geotechnical engineering to improve the engineering properties of weak soils. The use of geosynthetics such as geotextiles, geogrids, geomembranes, and geocells have been ever-increasing since their types and qualities have increased dramatically (Hataf *et al.* 2010). However, each geosynthetic product has different engineering properties depending on its effectiveness in certain geosynthetic functions such as separation, filtration, drainage, reinforcement, sealing, and protection. For instance, geogrids have been used for reinforcement in the construction of several earth-retaining and earth-supported structures (Das 2016). Moreover, they have been preferred by designers to support some foundations resting on weak soils such as road embankments under repeatable traffic loads and machine foundations under vibration (Hataf *et al.* 2010).

The foundations of these type of structures mentioned above are subjected to a static load as well as a repeated load. The static load stems from a structure's own weight (i.e., the weight of machine and foundation) whereas the repeated load emerges from the activity (i.e., the action of the moving parts of the machine) over the foundations (Moghaddas Tafreshi and Dawson 2010). Therefore, the objective of this study has been to understand the effects of a combination of static and repeated loads on the behavior of a circular shallow foundation resting on geogrid-reinforced and unreinforced sandy soil with a relative density of 65% (RD). For this purpose, twenty large-scale laboratory tests were performed, and numerical models of the laboratory box tests were developed by using the finite element method (FEM) modeling approach, which is verified with one-dimensional site response analysis, and as a consequence of this effort that refers to the innovation of the study, the consistency between the results obtained from both methods is observed. In particular, the primary

*Corresponding author, Ph.D. Student
E-mail: mtolun@atu.edu.tr
[a]Ph.D. Student
[b]Ph.D.
[c]Professor, Ph.D.
[d]Abel Bliss Professor, Ph.D.

ISSN: 2005-307X (Print), 2092-6219 (Online)

objective of this research effort is to demonstrate the benefits of geogrid reinforcement application for a shallow foundation improvement type geotechnical problem both experimentally and numerically. Some variables, which affect the behavior of the whole system, are investigated including the number of the geogrid layers, the amplitude of repeated load, and the number of load cycles.

In recent years, use of geogrid-reinforced soils has been of wide interest to geotechnical engineers with many studies that focused on the improvement of the load-bearing behavior of shallow foundations subjected to the static loads (Asakereh *et al.* 2013). Yet, there are relatively fewer studies on the load-bearing responses of shallow foundations resting on weak soils improved by geogrid reinforcement subjected to the dynamic loads. Although the latter topic is a more difficult task owing to the nature of the dynamic load, there are pertinent studies related to this topic in the literature such as Yeo *et al.* (1993), Shin *et al.* (2002), El Sawwaf and Nazir (2010), Alam *et al.* (2018), Wang *et al.* (2018), Useche-Infante *et al.* (2019). The main goal of this section is to present recent developments and current state of the art related to reinforced shallow foundations subjected to the dynamic loads.

Yeo *et al.* (1993) carried out some laboratory model tests to assess the cyclic load-induced settlement of a shallow foundation supported by sand reinforced with the geogrid layers. The results indicated that for obtaining the maximum bearing capacity for the sand-geogrid system tested, the optimum values of the total depth of geogrids and the width of geogrid, respectively, were about equal to 1.33B and 4B, where B refers to the width of the shallow foundation. Besides, it was stated that the geogrid reinforcement greatly reduced permanent deformation. Shin *et al.* (2002) presented some results of the large-scale laboratory model tests conducted to determine the permanent deformation of a sand soil due to the cyclic load, and the possibility of using 3 geogrid layers as the reinforcement to reduce settlement of the subgrade layer was investigated. The results showed that the accumulated permanent deformation due to cyclic loading was completed after the application of 10^5 load cycles. They also indicated that the soil became much stiffer because of the inclusion of the geogrid layers resulting in a decrease in the total accumulated permanent deformation. El Sawwaf and Nazir (2010) carried out a laboratory study to investigate the effect of geogrid reinforcement on the cumulative settlement of repeatedly loaded model footings placed on sand soil. The variables were the initial monotonic load levels, the number of load cycles, and the relative density of sand soil along with geogrid parameters including size and number of layers. The results indicated that for the same initial monotonic load and relative density of sand, the permanent deformation increased with the increase of the number of cycles. Additionally, it was mentioned that the geogrid length had to be greater than or equal to 5 times the footing width, and the recommended number of geogrid layers was equal to 3. Alam *et al.* (2018) performed large-scale tests to investigate the cyclic loading response of a model footing supported by a geogrid reinforced fill. The goal of the study was to evaluate the accumulation of permanent deformation of the footing constructed on a residual soil subjected to many load cycles. The results showed that both the permanent deformation of footing and the residual soil stress increased asymptotically with the increase of load cycles, and most of them occurred within the first few hundred load cycles. Therefore, it was stated that the first few hundred load cycles were particularly important for the accumulation of most of the soil permanent deformation. Wang *et al.* (2018) conducted seven sets of large-scale laboratory tests on a footing resting on geogrid-reinforced sand soil to examine the settlement response of the footings under cyclic loading. The results indicated that the ultimate bearing capacity of the footings increased with the increase of the geogrid numbers. Besides, it was stated that the depth of the first layer of geogrid was a critical factor to be considered in the design to increase the bearing capacity and avoid a punching shear type failure. Useche-Infante *et al.* (2019) examined the bearing capacity behavior of a circular footing resting on geogrid-reinforced sand soil by using laboratory model tests. The results showed that the improvement achieved depended on the relative density of sand because the bearing capacity increased when the value of this variable was increased. The improvement in the bearing capacity was also dependent on the location of the first geogrid layer, and the geogrid was more effective when it was installed within 0.25-0.40 times the circular footing diameter. Furthermore, the results indicated that the bearing capacity increased notably with the increase of the number of geogrid layers.

From the foregoing literature review, it can be understood that there are many factors that affect the bearing capacity of a shallow foundation resting on geogrid-reinforced sandy soils subjected to a combination of static and repeated loads. To reduce the burden of this study, the studies where optimum values were obtained for some variables such as the depth of the first layer of geogrid, the vertical distance of two geogrids and the length of the geogrid were taken into consideration. Additionally, only one type of geogrid, sandy soil with a relative density of 65%, and a single shallow foundation shape (i.e., circular) were considered in the scope. The variables investigated in the study both experimentally and numerically are the number of geogrid layers, the amplitude of repeated load, and the number of load cycles. Finally, a sinusoidal periodic harmonic load with 1 Hz frequency and different amplitudes was adopted as the applied repeated load. Consequently, a calibrated numerical study with one-dimensional site response analysis is included herein where the large-scale experimental study conditions are modeled exactly. Therefore, a calibrated numerical model with one-dimensional site response analysis can be shown as the advantage and innovation of the study. For this purpose, the performance of 2D dynamic site effects was calibrated with the 1D site effects obtained from the code of DEEPSOIL. It can be stated on behalf of the main contribution of numerical work that it is to indicate the deformed mesh outputs of the model including the geogrids for the variables considered in the study.

2. Materials and methods

2.1 Test apparatus

In this section, a brief explanation is given about the test apparatus. Fig. 1 shows a general view of the laboratory test setup, the test box itself, and all relevant attachments. The test box was designed as a steel frame with dimensions of 200 cm length, 200 cm height, and 200 cm width. There are two IPE 400 steel profiles over the test box to aid in moving the steel beam in one direction, and an actuator is mounted to this steel beam. The actuator was capable of applying dynamic loads with a maximum capacity of 260 kN via an electromechanical system which controlled repeated loading and produced desired load magnitudes and frequencies up to 20 Hz.

Fig. 1 General view of test apparatus and all relevant attachments

Fig. 2 Preparation of the first layer of sand bed with a relative density of 65% and vibratory compaction shown on top of wood pieces

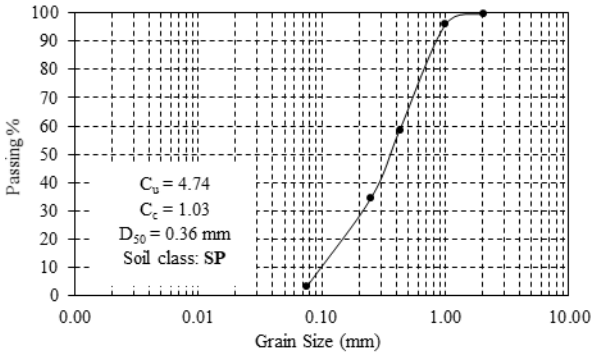

Fig. 3 Grain size distribution curve for the sand soil used

Table 1 Physical characteristics of geogrid reinforcement

Property	Value
Aperture shape	Triangular
Aperture size [mm]	33×33
Thickness [mm]	0.9
Junction efficiency [%]*	93
Isotropic stiffness ratio**	0.6
Tensile strength at strain 5% [kN/m]	200

*Load transfer capability, expressed as a percentage of ultimate tensile strength.

**The ratio between the minimum and maximum observed values of radial stiffness at 0.5% strain.

There are various methods for preparing a sand bed in the laboratory including impact, vibration, and the raining technique (i.e., pluviation). In preparing the box tests, it is important to have a uniform deposit to ensure the repeatability of tests (Asakereh *et al.* 2013). Among the mentioned methods, the vibration method was chosen appropriate for the dense sand condition in order to reach a desired relative density of sand.

The inner surfaces of the test box were marked at 0.1 m intervals for easing in preparation of the sand layers for the target density. The amount of sand for each layer was compacted by a hand-held vibratory compactor until the required layer height was achieved. To consistently achieve an in-place relative density of 65% uniformly with depth throughout the test box, the same compaction effort was applied on each layer of sand (Fig. 2). Coduto (2001) referred to sand soils with relative densities between 65% and 85% as “dense sands.” In accordance, to save time and labor during the vibratory compaction of the text box foundation, a sand bed was consistently prepared and used at this lower bound value of 65% in this study. Furthermore, pieces of wood each with dimensions of 198 cm length, 30 cm width and 2.5 cm thickness were used under the vibratory compactor to ensure uniform compaction and prevent breakage of sand grains during compaction, and all experiments were carried out under conditions where the water content was zero.

2.2 Description of materials

Sand samples were sieved from a predetermined batch of sieves according to the ASTM D 2487-11 standard specification. The grain size distribution obtained, and the sieve analysis test results are given in Fig. 3. Using the grain size distribution curve, the soil can be classified as poorly graded fine and clean sand (SP) according to Unified Soil Classification System (USCS). From the density bottle test, the specific unit weight of the test sand, γ_s was determined to be 26.7 kN/m^3. The minimum and maximum void ratios (e_{min} and e_{max}) of the sand were 0.518 and 0.762, respectively. The angle of internal friction of the sand was determined to be 40° from drained triaxial compression tests conducted on dry sand samples at a relative density of 65%.

As for geogrid reinforcement, all properties of which are

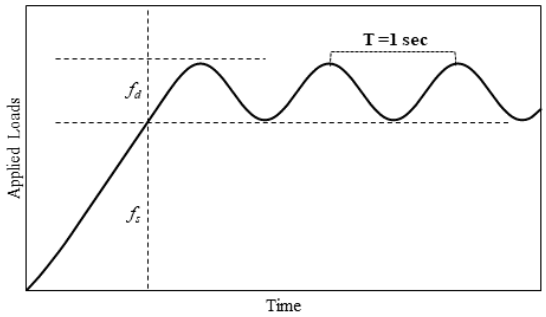

Fig. 4 Typical time history of initial static and dynamic loads

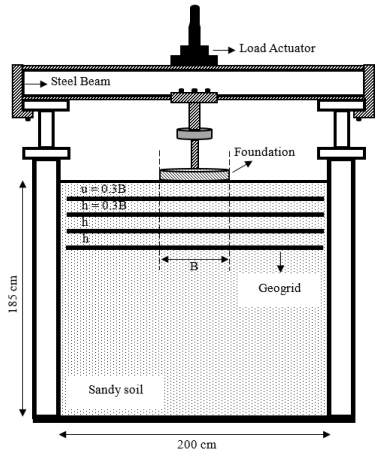

Fig. 5 View layout of actuator, geogrid, and circular shallow foundation

given in Table 1, a punched and drawn geogrid with triangular aperture (rip pitch 33 mm in longitudinal and diagonal) and radial tensile stiffness of 200 kN/m corresponding to 5% extension was employed. Note that for this type of geogrid, the tensile stiffness in each direction is identical therefore functioning equally in all directions.

2.3 Pattern of applied loads

The combination of static and dynamic loads used in experimental and numerical studies is given in Fig. 4.

In all cases, the shallow foundation is first subjected to a prespecified static load (f_s), afterwards, a repeated load derived in different proportions of the applied static load is superimposed to the static load. The proportions of the repeated load (f_d) were selected as 20%, 30%, and 50% of the prespecified static load which was obtained from the static test on the unreinforced sand soil. The reason why those proportions were chosen can be explained as each of the proportions represents a significant situation. For instance, the proportion values of the repeated load are assumed appropriate for expressing the stresses likely to be experienced under a traffic load or due to the loading of vibrating machines resting on foundations (i.e., the values of 20% and 30%), whereas the value of 50% represents an extreme occurrence (Moghaddas Tafreshi and Dawson 2010, Moghaddas Tafreshi and Dawson 2012, Asakereh *et al.* 2013). In addition to this, the repeated load with a frequency of 1 Hz was applied until the desired load cycle (up to 4998 cycles of loading and unloading for the experiments).

Table 2 Test Program

Test No	Load	Geogrid	N	f_d (%)	b/B	u/B	h/B
1	Static	No	0	-	-	-	-
2	Static	Yes	1, 2, 3, 4	-	6	0.3	0.3
3	Cyclic	No	0	20, 30, 50	-	-	-
4	Cyclic	Yes	1, 2, 3, 4	20, 30, 50	6	0.3	0.3

For the abbreviations such as N,B, b, u, and h in the table, please see testing program section

For precisely measuring the pattern of the applied loads on the foundation, load and displacement of the loading plate were measured during each test by a load cell with a capacity of 50 kN and a linearly variable differential transformer (LVDT) with an accuracy of 0.01% of the full range (100 mm).

2.4 Testing program

A series of experiments were planned and conducted so as to investigate the effect of the number of geogrid layers (N), the amplitude of repeated load, and the number of load cycles on the behavior of a circular shallow foundation resting on the sand soil with a relative density of 65%. The experiments were performed on reinforced and unreinforced sand in order to evaluate the improvements owing to the geogrids. The geometry of the test configurations examined in this study is given in Fig. 5. Additionally, the details of the testing program are given in Table 2.

In this study, the length of geogrid (*b*) is kept constant as 6B in all tests; where B refers to the width of the shallow foundation which is 30 cm in diameter with a circular cross-section. Different optimal values for the ratios of *b/B*, *u/B*, and *h/B* for optimizing the bearing capacity of shallow foundations were given in some previous studies (Chen *et al.* 2019, Dal *et al.* 2019). The distance between the first layer of geogrid and the foundation bottom is denoted by u, also h refers to the vertical distance between two geogrids. It is assumed that the ratio of *b/B* should be greater than 5-6 so that there is no influence on the foundation behavior (Fragaszy and Lawton 1984, Yoon *et al.* 2004, Ghazavi and Lavasan 2008, Asakereh *et al.* 2013). Yetimoglu *et al.* (1994) indicated that there was an optimum embedment depth for the first reinforcement layer at which the bearing capacity of a shallow foundation was the greatest. The tests showed that the optimum embedment depth was approximately *0.3B*. Besides, the optimum vertical distance between the two reinforcements was determined to be in the range of *0.2B-0.4B*. Mehrpazhouh *et al.* (2019) also showed that the optimum value of embedment depth of one reinforcement layer to reduce the soil deformation was approximately *0.3B*.

The test variables and the properties investigated in the experiments are mentioned as follows:

• The bearing capacity of a shallow foundation on sand with no geogrid under the static load,

• The effect of the number of geogrid layers on the behavior of the foundation under the static load,

• The effect of the number of geogrid layers on the behavior of the foundation under the repeated load,

The effects of both the amplitude of repeated load and the number of load cycles on the behavior of the foundation.

3. Findings and discussions

3.1 Experimental findings

In this section, the results obtained from the laboratory model tests are presented. An initial static test was performed first using the experimental setup of the shallow foundation resting on the sandy soil with no geogrid reinforcement to determine a reference load capacity. Secondly, the effect of the geogrid reinforcements in different numbers (i.e., up to 4 rows or layers) on the behavior of the shallow foundation was investigated to observe the improvement on the bearing capacity under both the static load and the repeated load. Finally, the effects of the repeated load (i.e., the effects of the amplitude of repeated load and the number of load cycles) on the geogrid reinforced sandy soil were studied in detail.

3.1.1 Unreinforced experiment results

The response of the shallow foundation resting on the unreinforced sandy soil under static load is shown in Fig. 6. This test was performed for determining the bearing capacity of unreinforced sandy soil, and for selecting a prespecified static load value to use in the tests in which the repeated load will be employed. Considering the variation of bearing capacity versus displacement behavior of the shallow foundation on the unreinforced soil in Fig. 6, no clear failure point was observed. In some cases, the plot of load-displacement takes almost a linear shape, and a value (i.e., load capacity) is never observed (Das 2017). The load capacity, in such case, is defined as the tangent intersection between the initial, stiff, straighter portion of the load-displacement curve and the steeper, straight portion of the curve (Adams and Collin 1997). Therefore, the bearing pressure of unreinforced sand was estimated to be approximately q_u=250 kPa, and this value was also accepted as the prespecified static load (see Fig. 6).

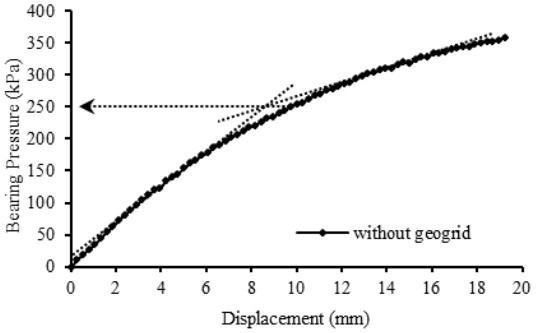

Fig. 6 Determination of the bearing pressure for unreinforced sand (considering Adams and Collin 1997)

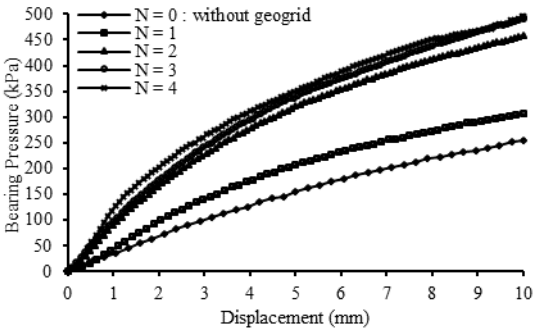

Fig. 7 Number of geogrid layers reducing the bearing pressure in case of static loading

3.1.2 Reinforced experiment results under static loading

To investigate the performance of the geogrid reinforcement under the static load, the bearing pressure values were recorded until a specific displacement of 10 mm in all cases where the number of geogrid layers considered was N=1, 2, 3, and 4 (see Fig. 7). This figure shows that the bearing pressure increases with the increase in the number of geogrids installed. There are several researchers in the literature that have reached this conclusion such as Yetimoglu *et al.* (1994), Laman and Yildiz (2003), Alamshahi and Hataf (2009), Vijaya and Gangadhara (2010), Badakhshan and Noorzad (2015), Biswas and Mittal (2017) and Ahmad *et al.* (2020). However, the optimum geogrid number is still controversial due to many factors that affect this phenomenon like the geogrid type, the location of the first geogrid layer, the vertical distance between two geogrids and the soil properties, etc. For instance, Moradi *et al.* (2018) stated that the degree of increase in bearing capacity depends on the vertical spacing of geogrid layers. Therefore, considering the studied conditions herein, the optimum number of geogrid layers is suggested to be 2, since there is no large increase in bearing pressure after 2 geogrid layers. Consequently, it is understood that employing 2 rows of geogrid would be more economical and effective to reduce the displacements of the shallow foundation in case of static loading conditions.

3.1.3 Reinforced experiment results under repeated loading

A series of experiments were carried out to examine the effects of the load duration and the number of load cycles of the repeated load, which were increased in different amplitude proportions of the bearing capacity, on the deformation behavior of the sandy soil. The results obtained from tests were presented in Figs. 8-10. Fig. 8 shows the results for the repeated load which is increased in the proportion of 20% of the bearing capacity. On the other hand, Figs. 9 and 10 indicate the results for the repeated loads which are increased in proportions of 30% and 50% of the bearing capacity, respectively. These figures indicate that the displacements increase with an increase in the number of cycles. They also show that the displacements of the shallow foundation increase rapidly in the first 100 load cycles in all cases. However, the rate of increase is reduced

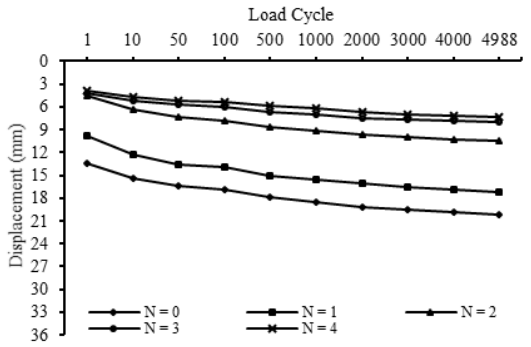

Fig. 8 Variations of displacement-load cycles for the proportion of dynamic load amplitude of 20% (N is the number of geogrid layers)

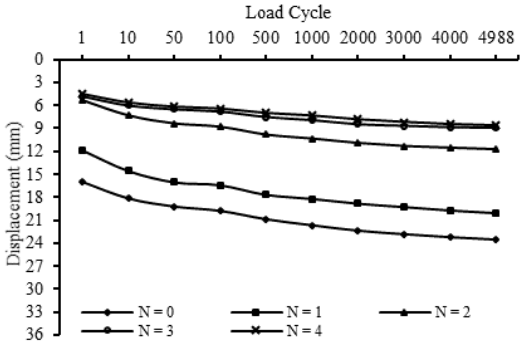

Fig. 9 Variations of displacement-load cycles for the proportion of dynamic load amplitude of 30% (N is the number of geogrid layers)

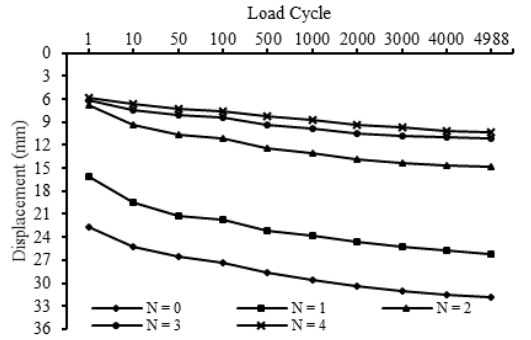

Fig. 10 Variations of displacement-load cycles for the proportion of dynamic load amplitude of 50% (N is the number of geogrid layers)

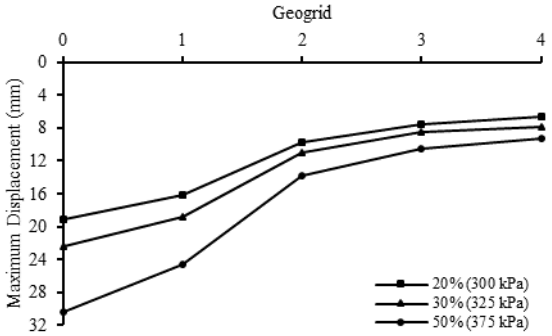

Fig. 11 Variations of the maximum displacement with different proportions of the repeated load for the number of load cycle of 2000

Table 3 Properties of sand for Mohr-Coulomb soil model

Parameter	Value
Dry unit weight of sand, γ_{dry} [kN/m^3]	17.60
Young's modulus, E [kN/m^2]	39000
Angle of internal friction, ϕ [º]	40
Angle of dilatancy, ψ [º]	10
Cohesion, c [kN/m^2]	0.1
Damping ratio, ξ [%]	5.0
Poisson's ratio, ν	0.2

Table 4 Model parameters employed for shallow foundation

Parameter	Value
Material type	Elastic
Unit weight, γ [kN/m^3]	77
Young's modulus, E [kN/m^2]	21×10^7
Plate thickness [m]	0.016
Plate diameter [m]	0.3
Poisson's ratio, ν	0.3

from 100 to 2000 load cycles and the displacements become negligible after then. This may be attributed to the soil densification owing to the sand soil particle rearrangements under the repeated loading-unloading process (Liu *et al.* 2016, Wang *et al.* 2018). It can be concluded that the sandy soil with a relative density of 65% used in this study behaves much stiffer after 2000 load cycles, specifically in the case of geogrid reinforcement cases. According to the study presented by Al-rkaby *et al.* (2017), most displacements accumulated during the first cycles when considering the cyclic behavior of geogrid-reinforced sand. With the increase in the number of cycles, deformation of sand soil increased moderately and then became constant.

As shown in Figs. 8-10, the displacement values of the shallow foundation decrease with the increase in the number of geogrid layers under the repeated load.

In particular, the displacements are reduced the most when the number of geogrid layers is equal to 2 or greater. However, there is no large decrease in displacement values after 2 geogrid layers, and this conclusion is valid for all the applied repeated load levels. Therefore, considering once again all the studied conditions herein, the optimum number of geogrid layers is again suggested to be 2 for the repeated loading. In conclusion, 2 rows of geogrid would be more economical and effective to reduce the displacements of the shallow foundation in cases of both static and dynamic loading conditions. Fig. 11 presents the shallow foundation test results for the different repeated load levels. The number of load cycle of 2000 was considered as a reference value in this figure since the displacements became negligible after that value in all proportions of the ultimate load level applied.

The displacements of the shallow foundation increase with the increase of the amplitude of the repeated load. Hegde and Sitharam (2016) reported that the damage caused to the foundation due to the cyclic loading reduces

as the amplitude of the vibration decreases. For instance, the displacements obtained when the proportion of the bearing capacity is equal to 50% are greater than those of 30%, but then the displacements obtained when the proportion is equal to 30% are greater than those of 20%. When the results are expressed numerically, it can be observed that the displacement value is calculated to be 9.68 mm while the number of geogrids and the proportionof bearing capacity are equal to 2 and 20%, respectively. On the other hand, for the same number of geogrid layers, the displacement values are calculated to be 10.92 mm and 13.80 mm when the proportions of the bearing capacity are equal to 30% and 50%, respectively. Finally, it can be stated that in the case of 2 rows of geogrids as compared to using no geogrid layer, the displacement of the shallow foundation decreases more than twice for all proportions of the repeated load.

3.2 Numerical modelling

Numerical models of the physical experiment were developed using the commercially available finite element software PLAXIS 2D. An initial static analysis was first performed using the finite element model of the shallow foundation resting on the sandy soil with no geogrid reinforcement to compare predictions with the experimental results. Secondly, the effect of the number of geogrid reinforcements on the behavior of the shallow foundation was investigated to observe the improvement on the bearing capacity under both the static load and the repeated load. Lastly, the effect of the repeated load (i.e., the effects of the amplitude of repeated load and the number of load cycles) on the geogrid reinforced sandy soil was studied in detail.

To provide more precise outputs, the element size had to be chosen as small as possible (Liu and Glass 2013). Therefore, a standard finite element fine mesh was chosen and used consistently in all analyses. The created finite element model with axial symmetry is presented in Fig. 12, and the numerical model consisted of 4112 elements and 35021 nodes. Furthermore, the required sand soil parameters belonging to the numerical model for the relative density of 65% were obtained from a series of laboratory tests as mentioned earlier in the materials description section (see Table 3).

The geogrids can be modelled by using special tension elements with a normal stiffness and no bending stiffness (Lee and Manjunath 2000). The “geogrid elements” were assigned adequately the tensile stiffness of 200 kN/m corresponding to 5% extension. On the other hand, the interaction between the geogrids and the surrounding sand soil was simulated by interface elements located between the geogrid and the soil elements. For properly modelling the frictional interactions between the contact surfaces, the interface elements are conveniently defined considering the relative density of sandy soil. In this study, the interaction between sandy soil and geogrids were simulated as nearly rigid contact friction. Finally, the circular shallow foundation was modelled by a “plate element” having the same properties of the steel plate used in the test (Table 4).

The finite element model boundary conditions were established with a relatively reliable artificial boundary

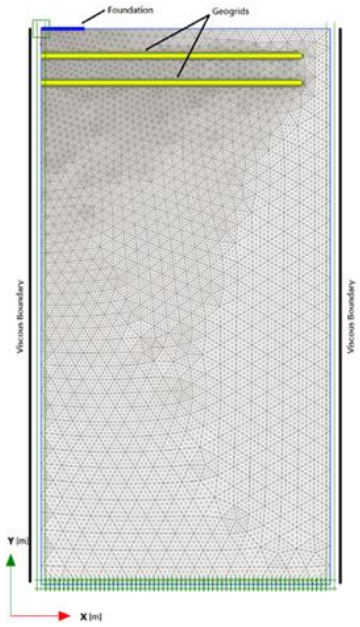

Fig. 12 The finite element model with 2 layers of geogrid shown with axial symmetry

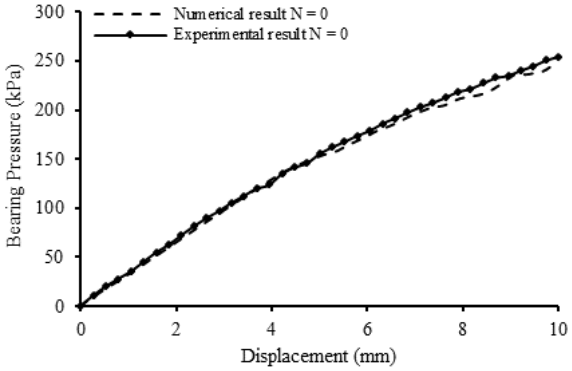

Fig. 13 Finite element model predictions compared to the experimental results for no geogrid case

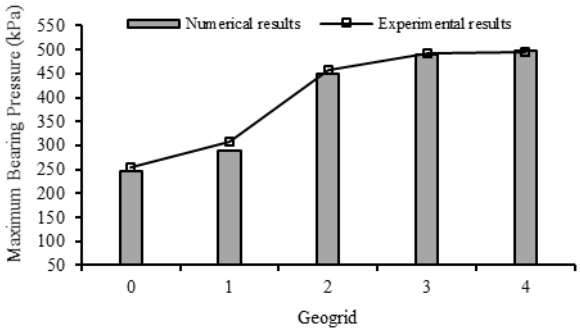

Fig. 14 Validation of the finite element model predictions for cases with different numbers of geogrid layers

called viscous boundary or dashpot boundary where the stress waves hitting the model boundaries because of the repeated load were damped without reflecting back due to damping. Therefore, as shown in Fig. 12, the viscous boundaries were defined at the vertical boundaries of the model, yet the horizontal boundaries of the model were free by the nature of the problem. The viscous boundary

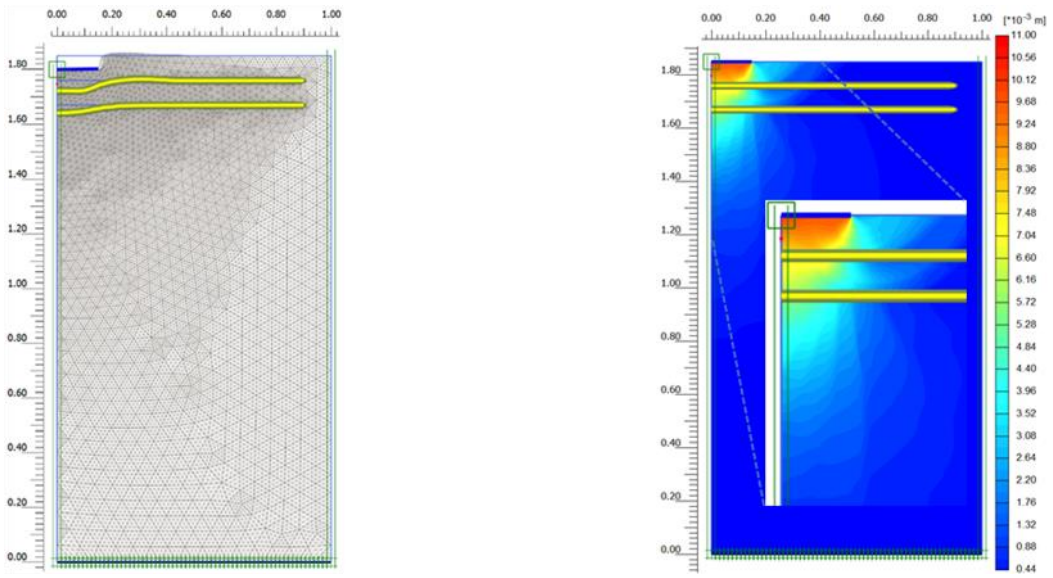

Fig. 15 The deformed finite element mesh (scaled up 5 times) and mobilized geogrids for the static load bearing analysis (contour plot shows vertical displacements)

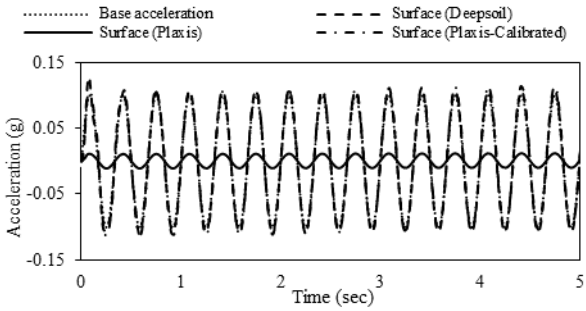

Fig. 16 Comparison of dynamic motions due to the 1D and 2D site response analysis

provides satisfactory responses for body waves because they absorb reflected energy with the advantage of using frequency independence to applied stresses (Cakir 2013).

3.2.1 Unreinforced numerical results

A comparison between the bearing pressure-displacement responses predicted using the finite element analyses and the results obtained from the experiments for unreinforced cases is shown in Fig. 13.

Considering the bearing pressure variation with displacements observed in the shallow foundation on the unreinforced soil, the finite element predictions are in good agreement with the experimental data and the established model reflects the test conditions fairly accurately.

3.2.2 Reinforced numerical results under static loading

To study the performance of the geogrid reinforcement under the static load, the bearing pressure values were calculated until a specific displacement of 10 mm in all cases where the number of geogrid layers considered was N=1, 2, 3, and 4, and then maximum bearing pressure values were determined. Afterwards, these numerical results were compared to the experimental data for model validation (see Fig. 14). The model predictions were found to be in good agreement with the test results, and this conclusion was valid for each case of the different number of geogrid layers.

As shown in Fig. 14, the bearing pressure increases with the increase in the number of geogrids installed. Like in the case of experimental findings, the optimum geogrid number is suggested to be 2, since there is no large increase in bearing pressure after 2 geogrid layers. Consequently, using 2 layers of geogrid, the displacements of the shallow foundation would be effectively reduced in case of static loading conditions. Moreover, the response of the model established by employing 2 geogrid layers is presented in Fig. 15. Note that the static load applied to the shallow foundation did not produce any appreciable displacement beyond the second layer of geogrid. Accordingly, two geogrid layers provide narrowing of the displacement contour in the horizontal direction.

3.2.3 Reinforced numerical results under repeated loading

In this section, a series of finite element analyses were performed to observe the effects of the load duration and the number of load cycles of the repeated load, which were increased in different proportions of the bearing capacity, as mentioned earlier, on the deformation behavior of the sandy

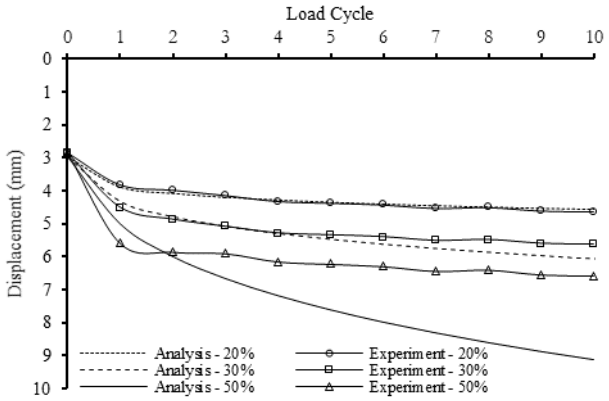

Fig. 17 Model predictions compared to experimental results in different proportions of the repeated load amplitude for the number of geogrid layers of 2

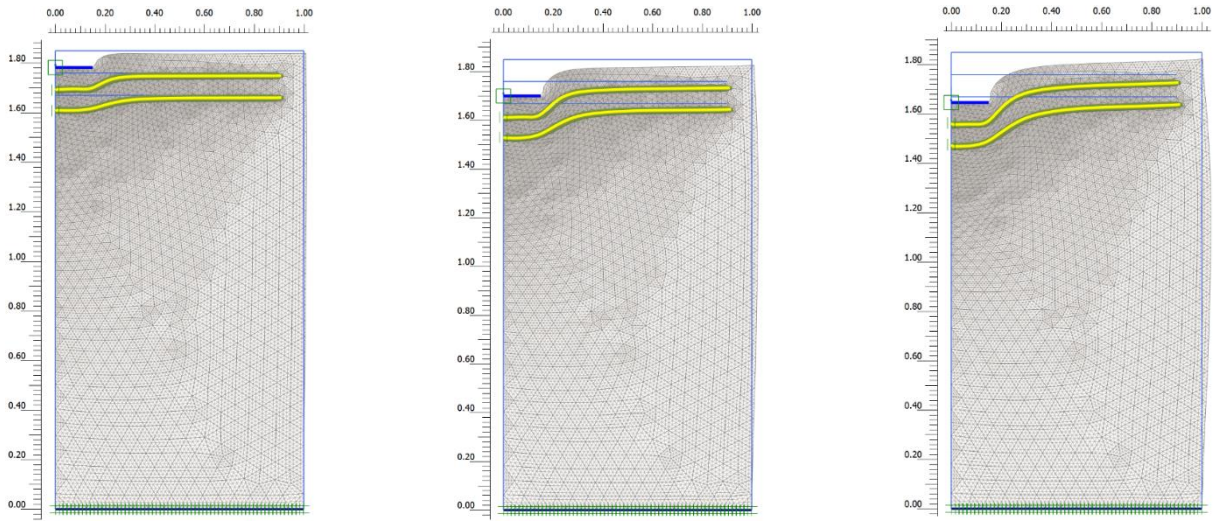

(a) f_d=20% (b) f_d=30% (c) f_d=50%

Fig. 18 The deformed finite element mesh after 10 load cycles for different proportions of the repeated load amplitude (Deformed mesh scaled up 5 times)

soil. Afterwards, the finite element results were compared with those of the experiments to check the performance of the numerical model for the dynamic loading conditions. Prior to the 2D numerical effort of the employed model throughout the study, it could be valuable to compare its site response performances with 1D analysis since the calibration of numerical model is quite an essential process. This comparison could be evaluated as a validation of the 2D numerical analysis. Therefore, in this study the performances of 2D dynamic site effects were compared with the 1D site effects obtained from the code of DEEPSOIL. It is reported that the code relatively enables to perform a 1D seismic site response analysis by equivalent linear and nonlinear behavior trends widely used in most of the practical applications (Musgrove *et al.* 2017). This capability of the code allows researchers to conduct large-scale simulations by capturing the effects of variability and uncertainty of soil, and dynamic motions. For comparison, a sinusoidal motion (vibration) with the maximum amplitude of 0.1 g and a frequency of 3 Hz (i.e., this value is equal to the natural frequency value of sandy soil) was applied to the sand from the base (bedrock) for 5 seconds. The surface responses of the sinusoidal motion by the site responses of the 1D and 2D analyses are illustrated below (Fig. 16).

From the plots, the 2D analysis yields lower results compared to the 1D analysis, and therefore 2D analysis results must be calibrated and the calibrated form of the 2D analysis result is given in the same plot. Thus, 2D-site effects can be considered as verified with 1D-site effects.

However, there are some limitations related to the numerical analyses such as analysis time and computer memory because dynamic analyses generally need more time and memory than static analyses. Hence, the duration of the repeated load was considered only for 10 seconds which means 10 load cycles because the frequency of load is equal to 1 Hz. For the reasons mentioned above, it was not possible to achieve the 4998 load cycles in the numerical study, unlike in the experiments.

Fig. 17 shows a comparison of the load cycle-displacement responses for different repeated load amplitude proportions calculated using the finite element analyses and the results obtained from the relevant model tests for reinforced cases with 2 geogrid layers. As seen in the figure, the finite element results match reasonably well

with the experimental data when the proportions of the repeated load are not too great such as 20% and 30%. On the other hand, it is observed that the agreement becomes the worst when the proportion of the repeated load reaches 50%.

As shown in Fig. 18, the displacements under the shallow foundation increase with the increase of the amplitude of the repeated load. For example, the displacements obtained when the proportion of the bearing capacity is equal to 50% are greater than those of 30%, but then the displacements obtained when the proportion is equal to 30% are greater than those for the 20%.

4. Limitations

The effectiveness of geogrid reinforcement in a shallow foundation application on sand soil subjected to a combination of static and dynamic loads is demonstrated in this paper. Although this is encouraging, it is necessary to mention that the results are obtained for only one type of geogrid, a sandy soil with a relative density of 65%, and a single shallow foundation shape (i.e., circular).

Furthermore, the shallow foundation was exposed to only one type of repeated load with a frequency of 1 Hz. However, a validated three-dimensional numerical model, which could consider the repeated load applied at different frequencies, would be extremely useful to evaluate any kind of problems such as machine foundations subjected to the effect of different vibrations.

Boundary dimensions of the substructure model under dynamic excitations are generally larger than static analysis. Otherwise, stress waves will be reflected leading to distortions in the computed results (Ordu and Ozkan 2006). Therefore, it is inevitable that the larger test box dimension is required for the larger foundation dimensions. And consequently, future studies may need to be carried out on larger-scale model foundations at various conditions where the foundations of different sizes, shapes, and depths can be employed

5. Conclusions

This paper focused on the beneficial use of geogrid reinforcement to increase the bearing capacity of a circular shallow foundation subjected to a combination of static and dynamic loads. In all cases, the shallow foundation is first subjected to a prespecified static load, after which a repeated load derived in different proportions of the applied static load is superimposed to the static load. The variables investigated in the study were the number of geogrid layers, the amplitude of repeated load, and the number of load cycles. Finally, for comparison with the experimental findings, calibrated numerical models of the physical experiments were established by using a 2D finite element modelling approach. The numerical results indicated good agreement with the test results throughout the study. The following are the detailed study findings:

1) An important improvement in the bearing capacity of sandy soil can be provided by employing geogrid reinforcement since the lateral restraint and interaction between geogrid and sandy soil reduce the vertical displacements below the foundation.

2) As the bearing capacity of sandy soil increased with the increasing number of geogrid layers installed in case of static loading, the bearing pressure–displacement behavior of the shallow foundation resting on geogrid-reinforced sandy soil is more rigid compared to unreinforced sandy soil.

3) Both from the experiments and the finite element predictions, the optimum number of geogrid layers was found to be 2 when there was no large increase in the bearing pressure after the placement of 2 geogrid layers in case of static loading conditions.

4) The displacement values of the shallow foundation decreased with the increase in the number of geogrid reinforcements under the repeated load conditions. In the case of 2 rows of geogrids as compared to using no geogrid layer, the displacement of the shallow foundation decreases more than twice for all proportions of the repeated load.

5) For all tests, the largest portion of the foundation displacement occurred after the first ten cycles, especially when the number of geogrids is 2 or more.

6) The displacements of the shallow foundation increased rapidly in the first 100 load cycles in all cases. However, the rate of increase was reduced from 100 to about 2000 load cycles; and the displacements became negligible after then.

7) Since the displacements under the shallow foundation increased with the increase in the proportion of the repeated load amplitude, the amplitude of the dynamic load is a considerable important parameter for the displacement behavior of shallow foundation.

8) Before numerical analyses are performed for dynamic loading conditions, the soil response of 2D analysis should be well calibrated with 1D site response analysis.

Acknowledgments

The authors would like to thank Republic of Turkey General Directorate of Highways and 5th Regional Directorate-Mersin for the supports which are required to be able to carry out the experimental part of the study.

References

Adams, M.T. and Collin, J.G. (1997), “Large model spread footing load tests on geosynthetic reinforced soil foundations”, *J. Geotech. Geoenviron. Eng.*, **123**(1), 66-72. https://doi.org/10.1061/(ASCE)1090-0241(1997)123:1(66).

Ahmad, H., Mahboubi, A. and Noorzad, A. (2020), “Scale effect study on the modulus of subgrade reaction of geogrid-reinforced soil”, *SN Appl. Sci.*, **2**(3), 1-22.. https://doi.org/10.1007/s42452-020-2150-4.

Alam, M.J.I., Gnanendran, C.T. and Lo, S.R. (2018), “Experimental and numerical investigations of the behavior of footing on geosynthetic reinforced fill slope under cyclic loading”, *Geotext. Geomembranes*, **46**(6), 848-859. https://doi.org/10.1016/j.geotexmem.2018.08.001.

Alamshahi, S. and Hataf, N. (2009), “Bearing capacity of strip footings on sand slopes reinforced with geogrid and grid-

anchor", *Geotext. Geomembranes*, **27**(3), 217-226. https://doi.org/10.1016/j.geotexmem.2008.11.011.

Al-rkaby, A.H., Chegenizadeh, A. and Nikraz, H.R. (2017), "Cyclic behavior of reinforced sand under principal stress rotation", *J. Rock Mech. Geotech. Eng.*, **9**(4), 585-598. https://doi.org/10.1016/j.jrmge.2017.03.010.

Asakereh, A., Ghazavi, M. and Moghaddas Tafreshi, S.N. (2013), "Cyclic response of footing on geogrid-reinforced sand with void", *Soils Found.*, **53**(3), 363-374. https://doi.org/10.1016/j.sandf.2013.02.008.

ASTM D2487-11 (2011), Standard practice for classification of soils for engineering purposes (Unified soil classification system), ASTM International, West Conshohocken, Pennsylvania, U.S.A.

Badakhshan, E. and Noorzad, A. (2015), "Load eccentricity effects on behavior of circular footings reinforced with geogrid sheets", *J. Rock Mech. Geotech. Eng.*, **7**(6), 691-699. https://doi.org/10.1016/j.jrmge.2015.08.006.

Biswas, S. and Mittal, S. (2017), "Square footing on geocell reinforced cohesionless soils", *Geomech. Eng.*, **13**(4), 641-651. https://doi.org/10.12989/gae.2017.13.4.641.

Cakir, T. (2013), "Evaluation of the effect of earthquake frequency content on seismic behavior of cantilever retaining wall including soil-structure interaction", *Soil Dyn. Earthq. Eng.*, **45**, 96-111. https://doi.org/10.1016/j.soildyn.2012.11.008.

Chen, J.F., Guo, X.P., Xue, J.F. and Guo, P.H. (2019), "Load behavior of model strip footings on reinforced transparent soils", *Geosynth. Int.*, **26**(3), 251-260. https://doi.org/10.1680/jgein.19.00003.

Coduto, D.P. (2001), *Foundation Design: Principles and Practices*, Prentice Hall, New Jersey, U.S.A.

Dal, K., Cansiz, O.F., Ornek, M. and Turedi, Y. (2019), "Prediction of footing settlements with geogrid reinforcement and eccentricity", *Geosynth. Int.*, **26**(3), 297-308. https://doi.org/10.1680/jgein.19.00008.

Das, B.M. (2016), "Use of geogrid in the construction of railroads", *Innov. Infrastruct. Solutions*, **1**(1), 15. https://doi.org/10.1007/s41062-016-0017-8.

Das, B.M. (2017), *Shallow Foundations: Bearing Capacity and Settlement*, CRC Press, Boca Raton, Florida, U.S.A.

El Sawwaf, M. and Nazir, A.K. (2010), "Behavior of repeatedly loaded rectangular footings resting on reinforced sand", *Alexandria Eng. J.*, **49**(4), 349-356. https://doi.org/10.1016/j.aej.2010.07.002.

Fragaszy, R.J. and Lawton, E. (1984), "Bearing capacity of reinforced sand subgrades", *J. Geotech. Eng.*, **110**(10), 1500-1507. https://doi.org/10.1061/(ASCE)0733-9410(1984)110:10(1500).

Ghazavi, M. and Lavasan, A.A. (2008), "Interference effect of shallow foundations constructed on sand reinforced with geosynthetics", *Geotext. Geomembranes*, **26**(5), 404-415. https://doi.org/10.1016/j.geotexmem.2008.02.003.

Hashash, Y.M.A., Musgrove, M.I., Harmon, J.A., Groholski, D.R., Phillips, C.A. and Park, D. (2015), *DEEPSOIL 6.1 User Manual*, University of Illinois at Urbana-Champaign, Illinois, U.S.A.

Hataf, N., Boushehrian, A.H. and Ghahramani, A. (2010), "Experimental and numerical behavior of shallow foundations on sand reinforced with geogrid and grid anchor under cyclic loading", *Scientia Iranica Trans. A Civ. Eng.*, **17**(1), 1-10.

Hegde, A. and Sitharam, T.G. (2016), "Behavior of geocell reinforced soft clay bed subjected to incremental cyclic loading", *Geomech. Eng.*, **10**(4), 405-422. https://doi.org/10.12989/gae.2016.10.4.405.

Laman, M. and Yildiz, A. (2003), "Model studies of ring foundations on geogrid-reinforced sand", *Geosynth. Int.*, **10**(5), 142-152. https://doi.org/10.1680/gein.2003.10.5.142.

Lee, K.M. and Manjunath, V.R. (2000), "Experimental and numerical studies of geosynthetic-reinforced sand slopes loaded with a footing", *Can. Geotech. J.*, **37**(4), 828-842. https://doi.org/10.1139/t00-016.

Liu, F.Y., Wang, P., Geng, X., Wang, J. and Lin, X. (2016), "Cyclic and post-cyclic behavior from sand–geogrid interface large-scale direct shear tests", *Geosynth. Int.*, **23**(2), 129-139. https://doi.org/10.1680/jgein.15.00037.

Liu, Y. and Glass, G. (2013), "Effects of mesh density on finite element analysis", *SAE Int.*, 2013-01-1375. https://doi.org/10.4271/2013-01-1375.

Mehrpazhouh, A., Moghaddas Tafreshi, S.N. and Mirzababaei, M. (2019), "Impact of repeated loading on mechanical response of a reinforced sand", *J. Rock Mech. Geotech. Eng.*, **11**(4), 804-814. https://doi.org/10.1016/j.jrmge.2018.12.013.

Moghaddas Tafreshi, S.N. and Dawson, A.R. (2010). "Behavior of footings on reinforced sand subjected to repeated loading–Comparing use of 3D and planar geotextile", *Geotext. Geomembranes*, **28**(5), 434-447. https://doi.org/10.1016/j.geotexmem.2009.12.007.

Moghaddas Tafreshi, S.N. and Dawson, A.R. (2012). "A comparison of static and cyclic loading responses of foundations on geocell-reinforced sand", *Geotext. Geomembranes*, **32**, 55-68. https://doi.org/10.1016/j.geotexmem.2011.12.003.

Moradi, G., Abdolmaleki, A., Soltani, P. and Ahmadvand, M. (2018), "A laboratory and numerical study on the effect of geogrid-box method on bearing capacity of rock-soil slopes", *Geomech. Eng.*, **14**(4), 345-354. https://doi.org/10.12989/gae.2018.14.4.345.

Musgrove, M., Harmon, J., Hashash, Y.M.A. and Rathje, E. (2017), "Evaluation of the DEEPSOIL software on the DesignSafe cyberinfrastructure", *J. Geotech. Geoenviron. Eng.*, **143**(9), 02817005. https://doi.org/10.1061/(ASCE)GT.1943-5606.0001755.

Ordu, E. and Ozkan, M.T. (2006), "Three-dimensional finite element analysis of the seismic behavior of pile foundations", *ITU Dergisi/d*, **5**(2), 27-34. (in Turkish).

PLAXIS 2D (2015), Geotechnical Finite Element Software Delft, The Netherlands. https://www.bentley.com/en/products/product-line/geotechnical-engineering-software/plaxis-2d.

Shin, E.C., Kim, D.H. and Das, B.M. (2002), "Geogrid-reinforced railroad bed settlement due to cyclic load", *Geotech. Geol. Eng.*, **20**(3), 261-271. https://doi.org/10.1023/A:1016040414725.

Useche-Infante, D., Aiassa Martinez, G., Arrúa, P. and Eberhardt, M. (2019), "Experimental study of behavior of circular footing on geogrid-reinforced sand", *Geomech. Geoeng.*, 1-19. https://doi.org/10.1080/17486025.2019.1683621.

Vijaya, S. and Gangadhara, S. (2010), "Experimental study on the performance of reinforced sand beds under repeated loads in presence of water", *Proceedings of the 5th International Conference on Recent Advances in Geotechnical Earthquake Engineering and Soil Dynamics*, San Diego, California, U.S.A., May.

Wang, J.Q., Zhang, L.L., Xue, J.F. and Tang, Y. (2018), "Load-settlement response of shallow square footings on geogrid-reinforced sand under cyclic loading", *Geotext. Geomembranes*, **46**(5), 586-596. https://doi.org/10.1016/j.geotexmem.2018.04.009.

Yeo, B., Yen, S.C., Puri, V.K., Das, B.M. and Wright, M.A. (1993), "A laboratory investigation into the settlement of a foundation on geogrid-reinforced sand due to cyclic load", *Geotech. Geol. Eng.*, **11**(1), 1-14. https://doi.org/10.1007/BF00452917.

Yetimoglu, T., Wu, J.T.H. and Saglamer, A. (1994). "Bearing capacity of rectangular footings on geogrid-reinforced sand", *J. Geotech. Eng.*, **120**(12), 2083-2099. https://doi.org/10.1061/(ASCE)0733-9410(1994)120:12(2083).

Yoon, Y.W., Cheon, S.H. and Kang, D.S. (2004), "Bearing capacity and settlement of tire-reinforced sands", *Geotext. Geomembranes*, **22**(5), 439-453. https://doi.org/10.1016/j.geotexmem.2003.12.002.

JS